

Original article

In print article

<https://doi.org/10.26565/2222-5617-2023-39-03>

UDC 539.232

PACS numbers: 81.15.-z; 81.07.-b; 87.85.J-; 81.05.-t

FUNCTIONAL CHARACTERISTICS OF HYDROXYAPATITE SINTERED AT HIGH TEMPERATURES

K.I. Sokol , R.V. Vovk 

V.N. Karazin Kharkiv National University, 4 Svobody Sq., 61022 Kharkiv, Ukraine

E-mail: sokolkarina8@gmail.com

Received on October 03, 2023. Reviewed on November 11, 2023.

Accepted for publication on November 17, 2023.

The functional characteristics of hydroxyapatite, which has carbonate impurities inside the hydroxyapatite crystal lattice after sintering in the temperature interval from room temperature to 1400 °C have been studied. It has been shown, that carbonate impurities are present in hydroxyapatite up to 1000 °C. Hydroxyapatite has a mixed AB-type of carbonate substitution. It has been shown, that all samples after the heating and sintering in the temperature interval from room to 1400 °C contain single phase hydroxyapatite. The samples have density greater than 95% of the theoretical for hydroxyapatite at the temperature of 1200 °C. The active shrinkage of the samples starts at temperature near 700 °C and reaches the maximum value at 1280 °C. The same tendency was demonstrated by the dependence of Vickers microhardness on sintered temperature. The maximum Vickers microhardness of 5.5 GPa was obtained in this work on the samples of hydroxyapatite after sintering at the temperature of 1100 °C. The mechanisms of the hydroxyapatite sintering at 1150 °C have been studied.

It has been shown, that the diffusion during the sintering of the samples is realized by the mechanism of lattice diffusion from the surface, as well as through the grain boundary diffusion in the polycrystalline hydroxyapatite. The microstructure of the hydroxyapatite particles after heating at high temperatures was studied. It has been shown, that at the initial stage of the sintering of hydroxyapatite, active mass transfer take place, which at the temperature of 1000 °C leads to the sintering of the particles with neck formations between them. The Arrhenius plot of the size of hydroxyapatite particles as a function of the heating temperature was obtained. The activation energy for diffusion processes in the particles at different temperatures was calculated. The obtained values were 36, 83, 5.11 and 11.28 kcal/mol at different intervals for the heating of hydroxyapatite.

Key words: *hydroxyapatite, phase composition, microstructure, shrinkage, density, microhardness, sintering, diffusion processes.*

In cites: *K.I. Sokol, R.V. Vovk. Functional characteristics of hydroxyapatite sintered at high temperatures. Journal of V. N. Karazin Kharkiv National University. Series Physics. Iss. 39, 2023, 40–46. <https://doi.org/10.26565/2222-5617-2023-39-03>*

INTRODUCTION

Calcium phosphate materials represent a class of compounds widely used in medicine, science and technology. Hydroxyapatite (HA) is a mineral component of hard tissues of humans and animals. For this reason, it is commonly applied in medical practice as an implant material [1]. There are several ways for HA production [2–5]. The simplest and cheapest is the HA synthesis by the precipitation from an aqueous solutions [6]. The resulting product is very often non-stoichiometric by the phase composition, which leads to the complex dependences of the functional characteristics on various factors. HA dense samples are usually produced by pressing of the synthesized powders after the purification them from impurities and heating (sintering) at the definite temperatures, holding time, heating and cooling rates. The data in literature describes the dependences of functional characteristics such as density, linear and volume shrinkages, Vickers microhardness, compressive strength, crack resistance and fracture toughness of HA samples on the heating temperature [7–12]. Most of these works focused on the improvement of quantitative characteristics using various sintering techniques, preliminary heat treatment and sintering duration [13–15]. At the same time, in these works little attention is paid to the impurities in the samples. In addition, the mechanisms of sintering of HA ceramics and calcium phosphates have been studied not enough. Nevertheless, this aspect is very important from the point of view of the understanding of the fundamental physical principles of densification and sintering of biomaterials used for medical applications.

The aim of this work was to study the functional characteristics of HA samples with impurities after heating in the temperature interval from room to 1400 °C, as well as the diffusion mechanisms during mass transfer and sintering of HA ceramics.

MATERIALS AND METHODS

HA was synthesized by the precipitation method from the aqueous solution according to the chemical reaction [6]:



The ratio of chemical reagents for the synthesis reaction was chosen to obtain a stoichiometric Ca/P ratio consist of 1.67. HA synthesis was carried out at 20 °C for 24 hours. The obtained precipitate was purified in distilled water four times to remove nitrate impurities. The resulting product was dried at room temperature for three days. The dried samples were ground into powders and sifted through a 100 µm sieve. Cylindrical samples with a diameter of 7 and a height of 4 mm were produced from the resulting

powders by pressing in a steel mold under the pressure of 100 MPa. The obtained compacts were heated in a muffle furnace in the temperature interval from room to 1400 °C with holding at definite temperature for 1 h. XRD patterns were collected from the resulting samples for phase identification. They were recorded using DRON-2.0 X-ray diffractometer in copper K α radiation (accelerating voltage 40 kV, anode current 10 mA) in the interval of diffraction angles 2 θ : 25 – 50°. The XRD patterns of the samples were compared with the standard samples from the ICDD powder diffraction database [10]. IR spectroscopy of the samples was carried out by mixing 1 mg of the sample with 100 mg of KBr, followed by pressing the mixture into transparent tablets. The spectra were carried out using an FTIR spectrometer SPECORD 75IR (Germany) in the wavenumber interval 400 – 4000 cm⁻¹. The impurity composition of the initial powder was studied using mass spectrometry of the gaseous products produced by heating of the samples in the temperature interval from room to 1000 °C. It was used MX-7304 mass spectrometer in the interval of mass numbers M/Z: 1 – 100 a.m.u. Density, linear and volume shrinkage, and Vickers microhardness were measured on the samples after heating at different temperatures. To study the diffusion processes occurring during the sintering of the samples, the linear and volume shrinkage were defined after the sintering of the samples at 1150 °C with different holding time.

The microstructure of the samples was studied using the scanning electron microscope LEO 1530 Gemini SEM (Germany) with accelerating voltage 30 kV. To ensure the drain of electrons from the surface of dielectric materials, the film consisting of Au and Pd were sputtered on the surface of the samples.

RESULTS AND DISCUSSION

Fig. 1 shows XRD patterns of the samples sintered at different temperatures.

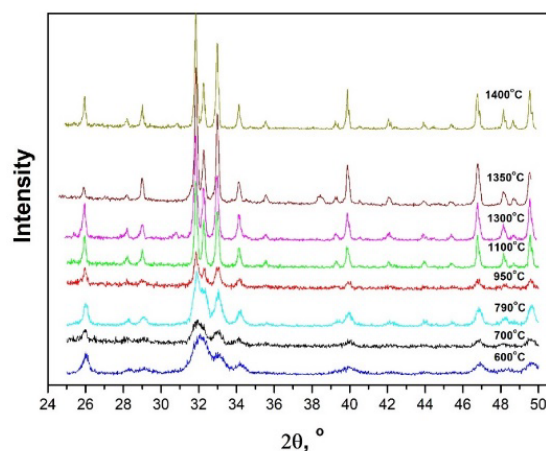


Fig. 1. X-ray diffraction patterns of the samples sintered at different temperatures.

They demonstrate that the initial samples have broadened diffraction lines in the diffraction angle interval 2θ : $30 - 35^\circ$. Such XRD patterns are characteristic for nanocrystalline calcium phosphate materials. While the heating temperature increases, the full width at half maximum (FWHM) of the lines on the XRD patterns decreases. This gives possibility to do the phase identification. According to the obtained results, the samples contain single phase HA (PDF № 9-432) [10]. The phase composition of the sintered samples does not change drastically with increasing of heating temperature. Figure 2 shows the IR spectra of the samples after heating at different temperatures.

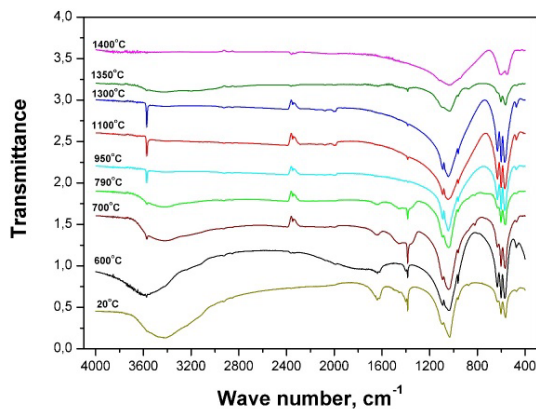


Fig. 2. IR spectra of the samples after heating at different temperatures.

The spectrum of the initial sample (20°C) contains absorption bands assigned to NO_3^- ions at 1385 cm^{-1} , as well as bands in the interval $1400 - 1550\text{ cm}^{-1}$ corresponded to the CO_3^{2-} ions located inside the HA crystal lattice in A- and B-positions [2]. The presence of NO_3^- ions on the IR spectra is the result of the presence of nitrate impurities in the initial (synthesized) HA samples. These impurities arise from the HA synthesis [6]. They decompose during the heating of the samples above 400°C . CO_3^{2-} ions (Fig. 2) are present inside the HA crystal lattice up to 1000°C . These data are also confirmed by the results of mass spectrometry of the gaseous products releasing from the initial HA samples at heating in the temperature interval from room to 1000°C (Fig. 3).

The spectra contain the emission peaks of gaseous products with mass numbers $M/Z = 18$ (H_2O), 30 (NO) and 44 (CO_2). The intense release of water (H_2O) from the samples in the temperature interval from room to 400°C is associated with the desorption of H_2O molecules from the surface of HA nanoparticles, as well as water chemically bound to the surface of HA particles and water molecules located inside the HA crystal lattice. In the temperature interval $400 - 600^\circ\text{C}$, an intense peak of NO release ($M/Z = 30$) is observed, which is associated with the

presence of nitrate impurities in the samples. These impurities are NH_4NO_3 (by-product) and $\text{Ca}(\text{NO}_3)_2$ which was not reacted during the HA synthesis. The release of CO_2 ($M/Z = 44$) occurs in three temperature intervals: from room to 400 , $400 - 550$ and $700 - 1000^\circ\text{C}$. The first two maxima are associated with the desorption of CO_2 adsorbed on the surface of HA nanoparticles.

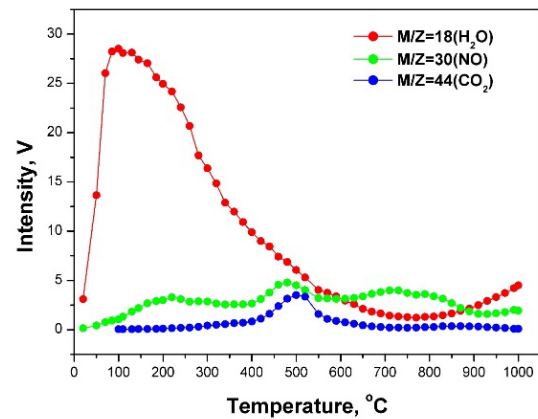


Fig. 3. Mass spectrometry of the release of gaseous products from the initial HA samples at heating in the temperature interval from room to 1000°C .

The peak of CO_2 release in the temperature interval from 700 to 1000°C is associated with the decomposition of CO_3^{2-} ions and the release of CO_2 from the HA lattice. The decomposition processes of impurities during the heating of the HA samples lead to the non-monotonic dependences of linear and volume shrinkage, as well as density and Vickers microhardness of the samples on the sintering temperature (Fig. 4 – 7).

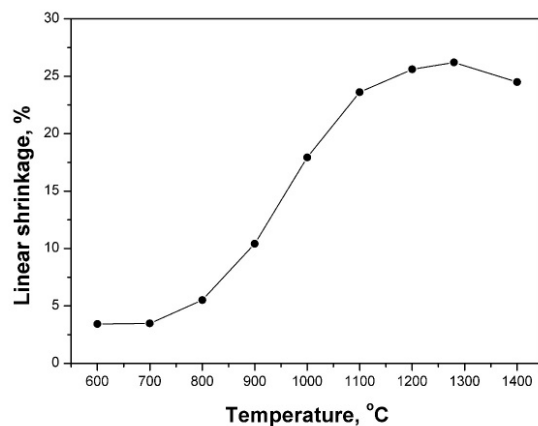


Fig. 4. Linear shrinkage of the samples after heating at different temperatures.

The density of the studied samples (Fig. 6) reaches its highest value of 3.05 g/cm^3 at 1300°C . In this case, the Vickers microhardness of the samples (Fig. 7) become the

maximum of 5.50 GPa at 1100 °C. The decrease in the density and Vickers microhardness of the samples (Fig. 6,7) could be explained by the formation of secondary phases such as α - and β -tricalcium phosphate (α -, β -Ca(PO₄)₂) as a result of the thermal decomposition of HA at high temperatures [10]. The amount of secondary phases

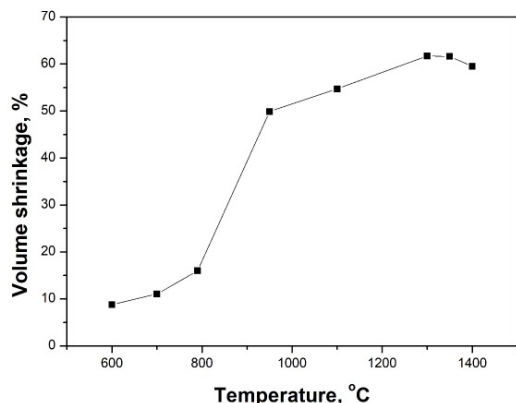


Fig. 5. Volume shrinkage of the samples after heating at different temperatures.

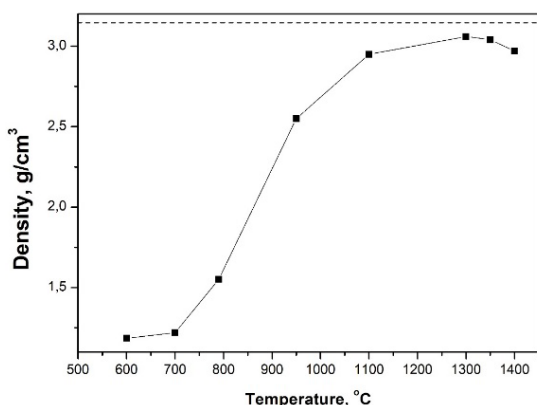


Fig. 6. Density of the samples after heating at different temperatures.

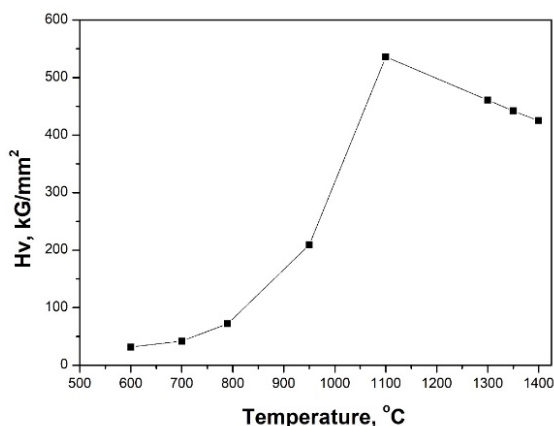


Fig. 7. Vickers microhardness of the samples after heating at different temperatures.

formed is beyond the sensitivity of XRD phase identification and therefore there are no diffraction lines of the corresponding phases on the XRD patterns (Fig. 1). To clarify the diffusion mechanisms responsible for the densification and sintering of the samples, the sintering of samples at 1150 °C with different duration of sintering have been performed. The results were shown in Fig. 8 and 9. For this, the shrinkage curves were approximated (curve fitting) by function:

$$y = a + bx^c, \quad (2)$$

where y – linear shrinkage, x – time of sintering at constant temperature, a , b , c – constant parameters. The results have demonstrated that the dependences of the linear shrinkage of the samples are well approximated simultaneously by the functions \sqrt{t} and $\sqrt[3]{t}$, where t is the heating time.

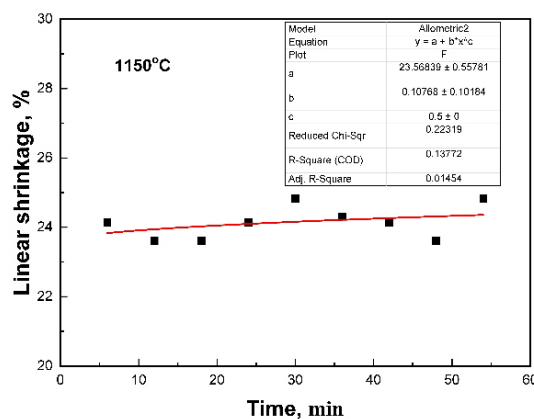


Fig. 8. Dependence of linear shrinkage of the samples on heating time at 1150 °C (fitting as \sqrt{t}).

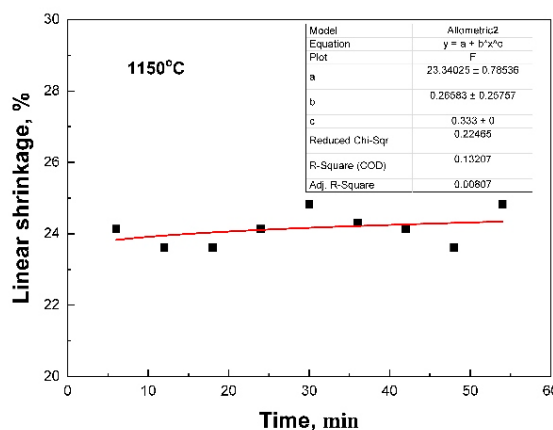


Fig. 9. Dependence of linear shrinkage of the samples on heating time at 1150 °C (fitting as $\sqrt[3]{t}$).

This indicates that the sintering of the samples governed by the mechanisms of lattice diffusion from the surface and grain boundary diffusion [16–19]. Fig. 10

shows SEM image of the samples obtained after the heating at different temperatures. It can be seen that the initial powder consists of nanoparticles ranging in the size from 10 to 50 nm. Mass transfer in the samples increases (600 – 700 °C) with the heating temperature. Sintering begins at temperatures of about 800 °C and at 950 °C the contacts between particles are formed. Sintered HA ceramics are formed at temperatures interval from 1000 to 1300 °C with the formation of closed isolated pores. The

increase in the heating temperature has results in the increase in the sizes of crystallites in the samples (Fig. 11). This give possibility to calculate the Arrhenius plot, which represents the dependence of the log of the crystallite size on the inverse heating temperature (Fig. 12). The activation energies of the sintering process in the samples were calculated by means of the Arrhenius plot. The obtained values can be divided into three temperature ranges: a) 600 – 790 °C, b) 790 – 1100 °C, c) 1100 – 1400 °C.

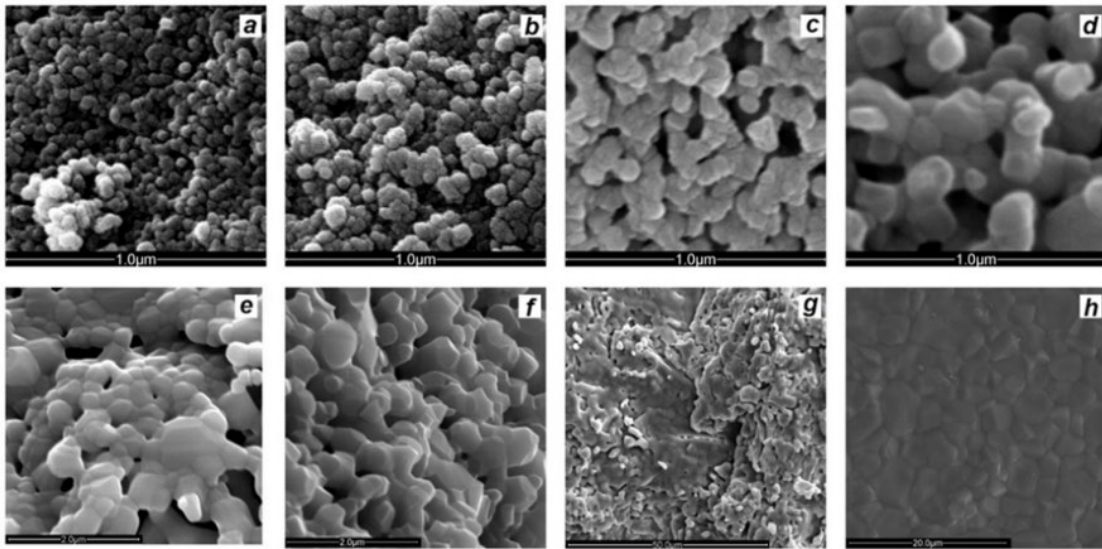


Fig. 10. SEM image of the samples obtained after heating at different temperatures. a) 600, b) 790, c) 950, d) 1100, e) 1300, f) 1350, g) 1400°C.

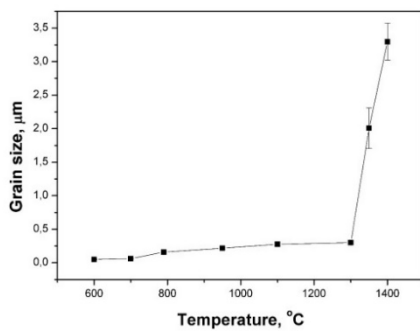


Fig. 11. Dependence of crystallite sizes in the samples after heating at different temperatures.

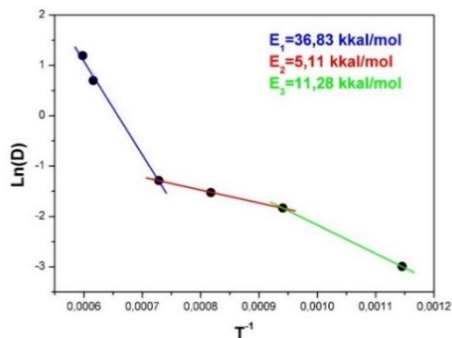


Fig. 12. Arrhenius plot of the crystallite size in the samples on the inverse heating temperature.

The calculated values of the activation energy in these intervals were: 11.28; 5.11; 36.83 kcal/mol. These values are in good agreement with similar results given in the literature [6, 10].

CONCLUSIONS

1. The functional characteristics of hydroxyapatite samples with impurities after heating in the temperature interval from room to 1400 °C were carried out.
2. The synthesized samples are nanocrystalline single phase hydroxyapatite.
3. The impurities present in the samples are NH_4NO_3 and $\text{Ca}(\text{NO}_3)_2$, as well as CO_3^{2-} ions located inside the HA crystal lattice. These impurities are formed at the stage of hydroxyapatite synthesis in the mother liquor.
3. Nitrate impurities are released from samples in the temperature range from room to 600 °C. CO_3^{2-} ions is stable in the HA crystal lattice up to the heating temperature of 1000 °C.
4. It has been shown that the non-monotonic dependences of linear and volume shrinkage, density and Vickers microhardness are associated with the presence of the impurities in the form of individual phases and in the form of ions located in the HA crystal lattice.

5. It has been shown that the sintering of hydroxyapatite samples occurs through the mechanism of lattice diffusion from the surface and grain boundary diffusion.

6. The activation energies of the growth of the hydroxyapatite crystallite during the heating of the samples were calculated. They were 11.28; 5.11 and 36.83 kcal/mol. The values of the activation energy are in good agreement with the data given in the literature for the growth of particles of calcium phosphate materials.

CONFLICT OF INTEREST

The authors declare that they no conflict of interest.

REFERENCES

1. L.L. Hench. J. Am. Ceram. Soc., 81, 1705 (1998). <https://doi.org/10.1111/j.1151-2916.1998.tb02540.x>
2. TSB Narasaraaju, DE Phebe. J. Mater. Sci., 31, 1 (1996). <https://doi.org/10.1007/BF00355120>
3. NASM Pu'ad, RHA Haq, H. Mohd Noh, HZ Abdullah, MI Idris, TC Lee. Materials Today: Proceedings, 29, 233 (2020). <https://doi.org/10.1016/j.matpr.2020.05.536>
4. K. Janakiraman, S. Swamiappan. Materials Letters, 357, 135731 (2024). <https://doi.org/10.1016/j.matlet.2023.135731>
5. S. Mondal, S. Park, J. Choi, T. T. H. Vu, V. H. M. Doan, T. T. Vo, B. Lee, J. Oh. Advances in Colloid and Interface Science, 321, 103013 (2023). <https://doi.org/10.1016/j.cis.2023.103013>
6. M. Jarcho, C. H. Bolen, M. B. Thomas, J. Bobick, J. F. Kay, R. H. Doremus, J. Mater. Sci. 11, 2027 (1976). <https://doi.org/10.1007/BF02403350>
7. A. J. Ruys, C. C. Sorrell, A. Brandwood. J Mater Sci Lett, 14, 744 (1995). <https://doi.org/10.1007/BF00253388>
8. G. Muralithran, S. Ramesh. Ceramics International, 26, 221 (2000). [https://doi.org/10.1016/S0272-8842\(99\)00046-2](https://doi.org/10.1016/S0272-8842(99)00046-2)
9. S. Ramesh, C. Y. Tan, R. Tolouei, M. Amiriyan, J. Purbolaksono, I. Sopyan, W. D. Teng. Materials and Design, 34, 148 (2012). <https://doi.org/10.1016/j.matdes.2011.08.011>
10. P. V. Landuyt, F. Li, J. P. Keustermans. J Mater Sci: Mater Med 6, 8 (1995). <https://doi.org/10.1007/BF00121239>
11. N. Thangamani, K. Chinnakali, F. D. Gnanam. Ceramics International, 28, 355 (2002). [https://doi.org/10.1016/S0272-8842\(01\)00102-X](https://doi.org/10.1016/S0272-8842(01)00102-X)
12. H.Y. Juang, M.H. Hon. Biomaterials, 17, 2059 (1996). [https://doi.org/10.1016/0142-9612\(96\)88882-X](https://doi.org/10.1016/0142-9612(96)88882-X)
13. J. Song, Y. Liu, Y. Zhang, L. Jiao. Materials Science and Engineering A, 528, 5421 (2011). <https://doi.org/10.1016/j.msea.2011.03.078>
14. Dj. Veljović, I. Zalite, E. Palcevskis, I. Smiciklas, R. Petrović, Dj. Janačković. Ceramics International, 36, 595 (2010). <https://doi.org/10.1016/j.ceramint.2009.09.038>
15. B. J. Babalola, O. O. Ayodele, P. A. Olubambi. Heliyon, 9, e14070 (2023). <https://doi.org/10.1016/j.heliyon.2023.e14070>
16. Z. He, J. Ma, C. Wang. Biomaterials, 26, 1613 (2005). <https://doi.org/10.1016/j.biomaterials.2004.05.027>
17. E. Landi, A. Tampieri, G. Celotti, S. Sprio. Journal of the European Ceramic Society, 20, 2377 (2000). [https://doi.org/10.1016/S0955-2219\(00\)00154-0](https://doi.org/10.1016/S0955-2219(00)00154-0)
18. S.J.L. Kang. Sintering, Densification, Grain Growth, and Microstructure. Butterworth-Heinemann (2005), 265 p. <https://doi.org/10.1016/B978-0-7506-6385-4.X5000-6>
19. J. S. Moya, C. Baudin, P. Miranzo. In Encyclopedia of Physical Science and Technology, ed. by R. A. Meyers, Academic Press (2003), p.865-878. <https://doi.org/10.1016/B012-227410-5/00694-3>

ФУНКЦІОНАЛЬНІ ХАРАКТЕРИСТИКИ ГІДРОКСИЛАПАТИТУ ПІСЛЯ ВІДПАЛУ ПРИ ВИСОКИХ ТЕМПЕРАТУРАХ

К.І. Сокол, Р.В. Вовк

*Харківський національний університет імені В.Н. Каразіна, 4 майдан Свободи., 61022 Харків, Україна
E-mail: sokolkarina8@gmail.com*

Надійшла до редакції 03 жовтня 2023 р. Переглянуто 11 листопада 2023 р.
Прийнято до друку 17 листопада 2023 р.

Досліджено функціональні характеристики зразків гідроксилапатиту, які містять карбонатні домішки в кристалічній решітці після відпалу в інтервалі температур від кімнатної до 1400 °С. Показано, що карбонатні домішки у зразках гідроксилапатиту присутні до температури 1000 °С. Гідроксилапатит має змішаний АВ-тип карбонатного заміщення. Показано, що всі зразки після відпалу в інтервалі температур від кімнатної до 1400 °С містять одну фазу гідроксилапатит. Зразки досягають щільності більше 95 % від теоретичної для гідроксилапатиту при температурі 1200 °С. При цьому активне ущільнення зразків починається за температур близько 700 °С і досягає максимуму при 1280 °С. Аналогічний хід демонструє залежність мікротвердості від температури відпалу. Максимальна твердість 5.5 ГПа була досягнута у даній роботі на зразках гідроксилапатиту після відпалу при температурі 1100 °С. Досліджено механізми спікання зразків за температури 1150 °С.

Показано, що дифузія при спіканні в досліджуваних зразках здійснюється механізмом поверхневої дифузії, а також через межі зерен в полікристалічних зразках гідроксилапатиту. Досліджено мікроструктуру зразків після відпалу при високих температурах. Показано, що на початковій стадії процесу спікання гідроксилапатиту відбувається активний масоперенос, який при температурі від 1000 °С призводить до спікання частинок з утворенням перешийок. Побудовано графік Арреніуса залежності розміру частинок гідроксилапатиту від температури відпалу. Обчислено енергію активації дифузійних процесів у зразках при різних температурах відпалу. Отримані значення склали 36, 83, 5.11 та 11.28 ккал/моль у різних інтервалах відпалу зразків гідроксилапатиту.

Ключові слова: *гідроксилапатит, фазовий склад, мікроструктура, усадка, щільність, мікротвердість, спікання, дифузійні процеси.*